EE5705 Electric Drives in Sustainable Energy Systems Course Project 2

Pei Xu

April 6, 2016

1 Introduction

This is the report of Course Project 2 for EE5705 Electric Drives in Sustainable Energy Systems. This report focuses on building the model of induction machines in dq domain and the model of controllers employing vector control theory in dq domain, as descibed in Chapter 3 and 5 in [2].

The report is recognized as the following. First, a detailed mathematical model of induction machines in dq domain is provided. Then, the report offers a modified mathematical model of induction machines and a model of two feedback loop controllers employing the vector control theory in dq domain. Finally, a set of simulation is conducted, in order to compare the induction machine model in dq domain and that in three-phase domain analyzed in Project 1, to compare the control effects of the controller model with and without voltage compensation, and to compare the control effects of the controller model with and without accurate parameters.

2 Mathematical Model of Induction Machine in dq Domain

2.1 Assumptions

Similarly to Project 1, the study to the model of induction machines are based on the below assumptions.

- The airgap is uniform.
- Eddy currents, friction and windage losses are all negligible.
- Stator and rotor windings are identical.
- The studied induction machine works under the condition in which the magnetic fields are unsaturated.
- The studied induction machine is magnetic linear.
- The studied induction machine has a squirrel-cage rotor.
- The input voltages and currents of the studied induction machine are sinusoidal balanced.

2.2 dq Winding Representation

For stator windings, in three-phase frame, assuming phase a is the reference phase, the stator current space vector $\vec{i}_s$ and the magnetomotive force space vector $\vec{F}_s$ at time t are defined as

$$\vec{i}_s^a(t) = i_a(t) + i_b(t)e^{j2\pi/3} + i_c(t)e^{j4\pi/3} \tag{2.1}$$

and

$$\vec{F}_s^a(t) = \frac{N_s}{p}\vec{i}_s^a(t) \tag{2.2}$$

where $i_a(t)$, $i_b(t)$ and $i_c(t)$ are the phase currents of the stator windings at time t, N_s is the equivalent turns of each stator winding, and p is the number of poles.

Supposing that the magnetomotive force at any instant time is produced by a group of two orthogonal windings, i_{sd} and i_{sq}, each of which has kN_s equivalent turns, then we have

$$\frac{kN_s}{p}(i_{sd}(t) + j\ i_{sq}(t)) = \frac{N_s}{p}\vec{i}_s^d(t) \tag{2.3}$$

where $\vec{i}_s^d$ is $\vec{i}_s$ using d-axis as the reference axis and is obtained as

$$\vec{i}_s^d(t) = \vec{i}_s^a(t)e^{-j\theta_{da}(t)} \tag{2.4}$$

in which $\theta_{da}(t)$ is the intersection angle between d-axis and a-axis at time t in electrical space.

Here we choose

$$k = \sqrt{3/2} \tag{2.5}$$

such that the winding magnetizing inductance in the dq domain satisfies

$$dq \text{ winding magnetizing inductance} = k^2 L_{m,1\phi} = L_m \tag{2.6}$$

where L_m is the per-phase magnetizing inductance in the three-phase frame, $L_{m,1\phi}$ is single-phase magnetizing inductance that is the same in both stator and rotor based on the assumptions.

Therefore, i_{sd} and i_{sq} can be obtained as

$$i_{sd} = \sqrt{\frac{2}{3}} \times Re\{\vec{i}_s^d(t)\} \tag{2.7}$$

and

$$i_{sq} = \sqrt{\frac{2}{3}} \times Im\{\vec{i}_s^d(t)\} \tag{2.8}$$

where $Re\{\vec{i}_s^d(t)\}$ and $Im\{\vec{i}_s^d(t)\}$ are respectively the real and imaginary part of $\vec{i}_s^d(t)$; and thus the relationship between dq currents and abc currents can be expressed as

$$\boldsymbol{i}_{s,dq} = \boldsymbol{T}_{s,abc\to dq}\boldsymbol{i}_{s,abc} \tag{2.9}$$

$$\boldsymbol{i}_{s,abc} = \boldsymbol{T}_{s,dq\to abc}\boldsymbol{i}_{s,dq} \tag{2.10}$$

where $\boldsymbol{i}_{s,abc} = \begin{bmatrix} i_a(t) \\ i_b(t) \\ i_c(t) \end{bmatrix}$, $\boldsymbol{i}_{s,dq} = \begin{bmatrix} i_{sd}(t) \\ i_{sq}(t) \end{bmatrix}$, $\mathbf{T_{s,abc\to dq}}$ and $\mathbf{T_{s,dq\to abc}}$ are the transformation matrices for stator windings that are obtained as

$$\boldsymbol{T}_{s,abc\to dq} = \sqrt{\frac{2}{3}} \begin{bmatrix} \cos(\theta_{da}(t)) & \cos(\theta_{da}(t) - 2\pi/3) & \cos(\theta_{da}(t) + 2\pi/3) \\ -\sin(\theta_{da}(t)) & -\sin(\theta_{da}(t) - 2\pi/3) & -\sin(\theta_{da}(t) + 2\pi/3) \end{bmatrix} \tag{2.11}$$

and

$$\boldsymbol{T}_{s,dq\to abc} = \sqrt{\frac{2}{3}} \begin{bmatrix} \cos(\theta_{da}(t)) & -\sin(\theta_{da}(t)) \\ \cos(\theta_{da}(t) - 2\pi/3) & -\sin(\theta_{da}(t) - 2\pi/3) \\ \cos(\theta_{da}(t) + 2\pi/3) & -\sin(\theta_{da}(t) + 2\pi/3) \end{bmatrix} \tag{2.12}$$

Similarly, for stator voltages, we have

$$\boldsymbol{v}_{s,dq} = \boldsymbol{T}_{s,abc\to dq}\boldsymbol{v}_{s,abc} \tag{2.13}$$

and

$$\boldsymbol{v}_{s,abc} = \boldsymbol{T}_{s,dq\to abc}\boldsymbol{v}_{s,dq} \tag{2.14}$$

where $\boldsymbol{v}_{s,dq} = \begin{bmatrix} v_{sd}(t) \\ v_{sq}(t) \end{bmatrix}$ and $\boldsymbol{v}_{s,abc} = \begin{bmatrix} v_a(t) \\ v_b(t) \\ v_c(t) \end{bmatrix}$.

For rotor windings, we have

$$\boldsymbol{i}_{r,dq} = \boldsymbol{T}_{r,ABC\to dq}\boldsymbol{i}_{r,ABC}, \quad \boldsymbol{v}_{r,dq} = \boldsymbol{T}_{r,ABC\to dq}\boldsymbol{v}_{r,ABC} \tag{2.15}$$

and

$$\boldsymbol{i}_{r,ABC} = \boldsymbol{T}_{r,dq\to ABC}\boldsymbol{i}_{r,dq}, \quad \boldsymbol{v}_{r,ABC} = \boldsymbol{T}_{r,dq\to ABC}\boldsymbol{v}_{r,dq} \tag{2.16}$$

where $\boldsymbol{i}_{r,dq} = \begin{bmatrix} i_{rd}(t) \\ i_{rq}(t) \end{bmatrix}$,$\boldsymbol{v}_{r,dq} = \begin{bmatrix} v_{rd}(t) \\ v_{rq}(t) \end{bmatrix}$,$\boldsymbol{i}_{r,ABC} = \begin{bmatrix} i_A(t) \\ i_B(t) \\ i_C(t) \end{bmatrix}$,$\boldsymbol{v}_{r,ABC} = \begin{bmatrix} v_A(t) \\ v_B(t) \\ v_C(t) \end{bmatrix}$,

$$\boldsymbol{T}_{r,ABC\to dq} = \sqrt{\frac{2}{3}} \begin{bmatrix} \cos(\theta_{dA}(t)) & \cos(\theta_{dA}(t) - 2\pi/3) & \cos(\theta_{dA}(t) + 2\pi/3) \\ -\sin(\theta_{dA}(t)) & -\sin(\theta_{dA}(t) - 2\pi/3) & -\sin(\theta_{dA}(t) + 2\pi/3) \end{bmatrix} \tag{2.17}$$

and

$$\boldsymbol{T}_{r,dq\to ABC} = \sqrt{\frac{2}{3}} \begin{bmatrix} \cos(\theta_{dA}(t)) & -\sin(\theta_{dA}(t)) \\ \cos(\theta_{dA}(t) - 2\pi/3) & -\sin(\theta_{dA}(t) - 2\pi/3) \\ \cos(\theta_{dA}(t) + 2\pi/3) & -\sin(\theta_{dA}(t) + 2\pi/3) \end{bmatrix} \tag{2.18}$$

in which $\theta_{dA}(t)$ is the intersection angle between d-axis and A-axis at time t in electrical space.

2.3 Flux Leakage Equation

Given that dq windings are orthogonal, there is no mutual inductance between d and q windings. Therefore, for stator windings, due to that the leakage flux caused by rotor currents does not cross the air gap, we have

$$\lambda_{sd} = (L_{ls} + L_m)i_{sd} + L_m i_{rd} \tag{2.19}$$

and

$$\lambda_{sq} = (L_{ls} + L_m)i_{sq} + L_m i_{rq} \tag{2.20}$$

where L_{ls} is the stator leakage inductance.

Similarly, for rotor windings, we have

$$\lambda_{rd} = (L_{rs} + L_m)i_{rd} + L_m i_{sd} \tag{2.21}$$

and

$$\lambda_{rq} = (L_{rs} + L_m)i_{rq} + L_m i_{sq} \tag{2.22}$$

where L_{rs} is the rotor leakage inductance.

Combining the above four equations, we obtain the flux leakage equation

$$\begin{bmatrix} \boldsymbol{\lambda}_{s,dq} \\ \boldsymbol{\lambda}_{r,dq} \end{bmatrix} = \begin{bmatrix} L_s & 0 & L_m & 0 \\ 0 & L_s & 0 & L_m \\ L_m & 0 & L_r & 0 \\ 0 & L_m & 0 & L_r \end{bmatrix} \begin{bmatrix} \boldsymbol{i}_{s,dq} \\ \boldsymbol{i}_{r,dq} \end{bmatrix} \tag{2.23}$$

where $L_s = L_{ls} + L_m$, $L_r = L_{lr} + L_m$ and $\boldsymbol{\lambda}_{s,dq} = \begin{bmatrix} \lambda_{sd}(t) \\ \lambda_{sq}(t) \end{bmatrix}$, $\boldsymbol{\lambda}_{r,dq} = \begin{bmatrix} \lambda_{rd}(t) \\ \lambda_{rq}(t) \end{bmatrix}$.

2.4 Voltage Equation

According to Ohm's law and Faraday's law, the stator voltage space vector can be expressed as

$$\vec{v}_s^a = R_s \vec{i}_s^a + \frac{d}{dt}\vec{\lambda}_s^a \tag{2.24}$$

where R_s is the equivalent resistance of each stator winding.

Therefore, we have

$$\vec{v}_s^d e^{j\theta_{da}} = R_s \vec{i}_s^d e^{j\theta_{da}} + \frac{d}{dt}(\vec{\lambda}_s^d e^{j\theta_{da}}) \tag{2.25}$$

Simplifying the above equation, we get

$$\begin{aligned} \vec{v}_s^d &= R_s \vec{i}_s^d + \frac{d\vec{\lambda}_s^d}{dt} + j\vec{\lambda}_s^d \frac{d\theta_{da}}{dt} \\ &= R_s \vec{i}_s^d + \frac{d\vec{\lambda}_s^d}{dt} + j\omega_d \vec{\lambda}_s^d \end{aligned} \tag{2.26}$$

where

$$\omega_d = \frac{d\theta_{da}}{dt} \tag{2.27}$$

Given that $\vec{v}_s^d = v_{sd} + j\ v_{sq}$, $\vec{i}_s^d = i_{sd} + j\ i_{sq}$ and $\vec{\lambda}_s^d = \lambda_{sd} + j\ \lambda_{sq}$ we have

$$\boldsymbol{v}_{s,dq} = R_s \boldsymbol{i}_{s,dq} + \frac{d}{dt}\boldsymbol{\lambda}_{s,dq} + \omega_d \begin{bmatrix} 0 & -1 \\ 1 & 0 \end{bmatrix} \boldsymbol{\lambda}_{s,dq} \tag{2.28}$$

Similarly, for rotor windings, we have

$$\boldsymbol{v}_{r,dq} = R_r \boldsymbol{i}_{r,dq} + \frac{d}{dt}\boldsymbol{\lambda}_{r,dq} + \omega_{dA} \begin{bmatrix} 0 & -1 \\ -1 & 0 \end{bmatrix} \boldsymbol{\lambda}_{r,dq} \tag{2.29}$$

where R_r is the equivalent resistance of each stator winding and

$$\omega_{dA} = \frac{d\theta_{dA}}{dt} \tag{2.30}$$

2.5 Torque Equation

Given that dq windings are orthogonal, the produced torque on the d-axis is caused by the the flux that is due to the q-axis winding. Referring to Chapter 10 of [1], we have

$$dT_{em,d}(\xi) = \left[\frac{p}{2} \cdot r \cdot (\widehat{B}_{rq} \cos\xi) \cdot l \cdot i_{rd} \cdot (\frac{\sqrt{3/2}N_s}{p} \cos\xi) \right] d\xi \tag{2.31}$$

where $\widehat{B}_{rq} \cos\xi$ is the flux density caused by rotor windings on q-axis at angle ξ, r is the rotor radius, and l is the length of rotor.

Therefore,

$$T_{em,d} = 2 \int_{\xi=-\pi/2}^{\xi=\pi/2} dT_{em,d}(\xi) = \frac{p}{2} \left(\pi \frac{\sqrt{3/2}N_s}{p} r l \widehat{B}_{rq} \right) i_{rd} \tag{2.32}$$

Given that $\widehat{B}_{rq} = \mu_0 \widehat{H}_{rq} = \mu_0 \frac{\widehat{F}_{rq}}{l_g}$, $\widehat{F}_{rq} = \left(\frac{\sqrt{3/2}N_r}{p} \right) \frac{\lambda_{rq}}{L_m}$ and $N_r = Ns$ where μ_0 is the permeability of air, l_g is the length of air gap, $\widehat{H}_{rq}$ is the peak filed intensity of rotor windings along the q-axis, $\widehat{F}_{rq}$ is the peak magnetomotive force of rotor windings along the q-axis, N_r is the equivalent turns of each rotor winding, and N_s is the equivalent turns of each stator winding, the above equation can be further simplied, and $T_{em,d}$ can be expressed as

$$T_{em,d} = \frac{p}{2}(L_m i_{sq} + L_r i_{rq}) i_{rd} = \frac{p}{2} \lambda_{rq} i_{rd} \tag{2.33}$$

Similarly, the produced torque on the q-axis can be expressed as

$$T_{em,q} = -\frac{p}{2}(L_m i_{sd} + L_r i_{rd}) i_{rq} = -\frac{p}{2} \lambda_{rd} i_{rq} \tag{2.34}$$

Therefore, the electromagnetic torque can be expressed as

$$T_{em} = T_{em,d} + T_{em,q} = \frac{p}{2}(\lambda_{rq} i_{rd} - \lambda_{rd} i_{rq}) \tag{2.35}$$

or

$$T_{em} = \frac{p}{2} L_m (i_{sq} i_{rd} - i_{sd} i_{rq}) \tag{2.36}$$

2.6 Angular Equations

The intersection angle between a-axis and A-axis in electrical radians, θ_m, satisfies

$$\theta_{dA} = \theta_{da} - \theta_m \tag{2.37}$$

and

$$\theta_m = \int \omega_m(t)dt + \theta_0 \tag{2.38}$$

where ω_m is the electrical rotational speed and θ_0 is the the initial angle by which rotor and stator coils are offset in electrical space.

Therefore, according to Eqn. 2.27 and 2.30 we have

$$\omega_d = \omega_{dA} + \omega_m \tag{2.39}$$

Based on the assumptions, we have

$$\frac{d\omega_{mech}}{dt} = \frac{T_{em} - T_L}{J} \tag{2.40}$$

where ω_{mech} is the mechanical rotational speed and T_L is the load torque and J is the moment of inertia.

Given that

$$\omega_m = \frac{p}{2}\omega_{mech} \tag{2.41}$$

where p is the number of poles of the given induction machine, we have the angular acceleration equation

$$\frac{d\omega_m}{dt} = \frac{p}{2}\frac{T_{em} - T_L}{J} \tag{2.42}$$

3 Vector Control in dq Domain

3.1 Selection of d-Axis

In this project, the direction of the space vector $\vec{B}_r$ is chosen as the d-axis. Therefore, we can keep $\vec{i}_s^a$ always ahead of $\vec{B}_r$ by 90° in the rotation direction through appropriately changing i_a, i_b and i_c, and, thereby, the induction machine can be controlled to emulate the performance of DC motor and the brushless DC motor drives.

Given that $\vec{B}_r$ and $\vec{\lambda}_r$ have the same direction, d-axis is also aligned to $\vec{\lambda}_r$. Hence, we have

$$\lambda_{rq} = 0 \tag{3.43}$$

From Eqn. 3.43 and the flux leakage equation, Eqn. 2.23, we have

$$\lambda_{rd} = L_r i_{rd} + L_m i_{sd} \tag{3.44}$$

and

$$i_{rq} = -\frac{L_m}{L_r} i_{sq} \tag{3.45}$$

From Eqn. 3.43 and 3.45, the torque equation, Eqn. 2.35, can be rewritten as

$$T_{em} = \frac{p}{2} \lambda \left(\frac{L_m}{L_r} i_{sq} \right) \tag{3.46}$$

Since the studied induction machine is assumed to have a squirrel-cage rotor, the rotor voltage is 0 and thus

$$v_{rd} = v_{rq} = 0 \tag{3.47}$$

.

Therefore, from Eqn. 3.43 and the voltage leakage equation, Eqn. 2.29, we have

$$\omega_{dA} = -R_r \frac{i_{rq}}{\lambda_{rd}} \tag{3.48}$$

Define

$$\tau_r \triangleq \frac{L_r}{R_r} \tag{3.49}$$

and thus, from Eqn. 3.45 and 3.48, ω_{dA} also can be expressed as

$$\omega_{dA} = \frac{L_m}{\tau_r \lambda rd} \tag{3.50}$$

From $v_{rd} = v_{rq} = 0$ and the voltage equation, Eqn. 2.28 and 2.29, we can infer out that λ_{rd} and i_{sd} satisfies

$$\frac{d\lambda_{rd}}{dt} + \frac{\lambda_{rd}}{\tau_r} - \frac{L_m}{\tau_r} i_{sd} \tag{3.51}$$

3.2 Measurement of Control Variables

In the control strategy mentioned in the last subsection, the control to induction machines are realized via adjusting the input stator currents in the dq domain. Therefore, the control variables are i_{sd} and i_{sq}. However, these two quantities are virtual and cannot be measured or controlled directly. Hence we need a model to calculate i_{sd}, i_{sq} and θ_{da} in order to obtain the desired stator currents in the three-phase frame.

For i_{sd} and i_{sq}, they can be obtained via Eqn. 2.9 where i_A, i_B and i_C are gotten via measurement.

In order to calculate θ_{da}, we need an ideal induction machine model whose structure is the same to that of the actual machine model and whose parameters are estimated according to the actual machine.

3.3 Controller Design

In the control strategy mentioned in the last subsection, i_{sd} is employed to maintain the peak value of $\vec{B}_r$ at its rated value; and i_{sq} is employed to deliver the desired electomganetic torque.

Therefore, the reference value of i_{sd} is its rated value, i.e.

$$i_{sd}^* = \sqrt{\frac{2}{3}} Re\{\vec{i}_{s,rated}^{\,d}\} \tag{3.52}$$

The reference value of i_{sq} is obtained through the speed loop, in which the mechanical rotation speed ω_{mech} is chosen as the input variable that can be measured directly and of which the reference value is its rated value. This loop is realized through a proportional-integral controller whose transfer function is

$$K_s(s) = \frac{K_{i,s}}{s} + K_{p,s} \tag{3.53}$$

where

$$K_{i,s} = \frac{\omega_c^2 J}{k\sqrt{1+\tan^2(PM)}} \tag{3.54}$$

and

$$K_{p,s} = \frac{K_{i,s}\tan(PM)}{\omega_c} \tag{3.55}$$

in which ω_c is the crossover frequency that is equal to the desired bandwidth numerically, and PM is the desired phase margin.

The applied voltages are obtained via the current loop, in which the reference value of i_{sd} and i_{sq}, i.e. i_{sd}^* and i_{sq}^*, are the reference input variables and i_{sd} and i_{sq} obtained via the measured stator currents are the feedback signals. This loop is also realized through a proportional-integral controller whose transfer function is

$$K_i(s) = \frac{K_{i,i}}{s} + K_{p,i} \tag{3.56}$$

where

$$K_{i,i} = \omega_c \sqrt{\frac{R_s^2 + (\omega_c L_s \sigma)^2}{1+\tan^2(PM - \pi/2 + \arctan(\omega_c L_s\sigma/R_s))}} \tag{3.57}$$

and

$$K_{p,i} = \sqrt{\frac{R_s^2 + (\omega_c L_s \sigma)^2}{1/(\tan^2(PM - \pi/2 + \arctan(\omega_c L_s\sigma/R_s))) + 1}} \tag{3.58}$$

in which

$$\sigma = 1 - \frac{L_m^2}{L_s L_r} \tag{3.59}$$

The current loop calculates v_{sd} and v_{sq} via

$$\boldsymbol{v}'_{s,dq} = R_s \boldsymbol{i}_{s,dq} + \sigma L_s \frac{d}{dt}\boldsymbol{i}_{s,dq} \tag{3.60}$$

whereas, from Eqn. 2.28 and 2.29,

$$\boldsymbol{v}_{s,dq} = R_s \boldsymbol{i}_{s,dq} + \sigma L_s \frac{d}{dt} \boldsymbol{i}_{s,dq} + \begin{bmatrix} 1 & 0 \\ 0 & \omega_d \end{bmatrix} \frac{L_m}{L_r} \boldsymbol{\lambda}_{r,dq} + \begin{bmatrix} -1 & 0 \\ 0 & 1 \end{bmatrix} \omega_d \sigma L_s \boldsymbol{i}_{s,dq} \tag{3.61}$$

Therefore, we need a voltage compensation model for the current loop and the reference applied voltage is obtained via

$$\boldsymbol{v}^*_{s,dq} = \boldsymbol{v}'_{s,dq} + \boldsymbol{v}_{s,dq,comp} \tag{3.62}$$

where, from Eqn. 3.61,

$$\boldsymbol{v}_{s,dq,comp} = \begin{bmatrix} 1 & 0 \\ 0 & \omega_d \end{bmatrix} \frac{L_m}{L_r} \boldsymbol{\lambda}_{r,dq} + \begin{bmatrix} -1 & 0 \\ 0 & 1 \end{bmatrix} \omega_d \sigma L_s \boldsymbol{i}_{s,dq} \tag{3.63}$$

4 Case Study

4.1 Specifications of the Studied Induction Machine

The studied case is based on a GE three phase induction machine. The involved specifications of this machine are listed in Table 1.

Table 1: Specifications of the Studied Induction Machine

Rated Frequency	60 Hz	R_s	1.4 mΩ
Rated Line Voltage	575 V	R_r	0.991 mΩ
Poles	6	X_{ls}	34 mΩ
Full Load Slip	1%	X_{lr}	31 mΩ
Moment of Inertia	75 kg·m^2	X_m	575 mΩ

4.2 Modeling of Studied Induction Machine in MATLAB/Simulink

The MATLAB/Simulink model of the studied machine in *dq* domain is shown in Fig. 1.

The complete model of the machine with speed and current loop controllers and voltage compensation is shown in Fig. 2, in which the Estimated Motor Model is the same to the Actual Motor Model except for that the estimated model does not have the components calculating $\boldsymbol{i}_{s,dq}$ and $\boldsymbol{i}_{r,dq}$ via $\boldsymbol{v}_{s,abc}$.

The details of the voltage compensation model is shown in Fig. 3.

4.3 Simulation and Numerical Analysis

4.3.1 Line Start Simulation

In this simulation, the machine is at the all-zero condition initially, and the balanced sinusoidal stator voltage with rated value is applied at the time $t = 0.2$s. No controller takes part in this course.

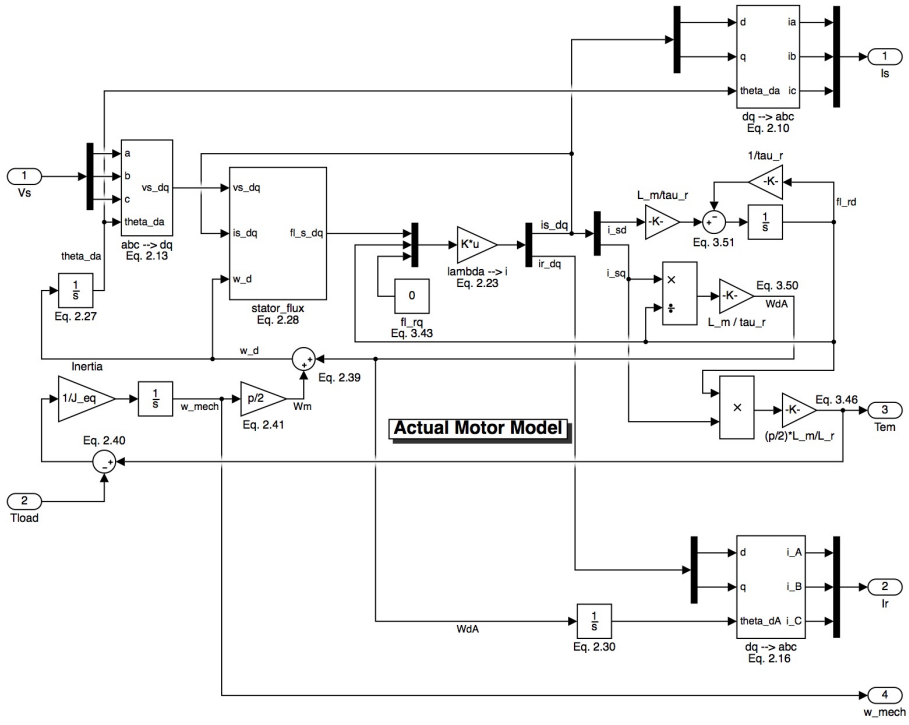

Figure 1: Model of Induction Machine in dq Domain

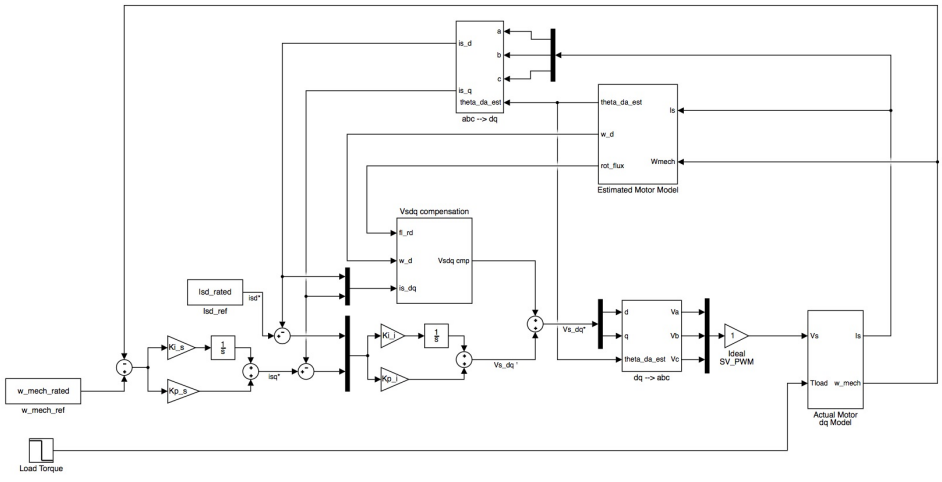

Figure 2: Model of Induction Machine with Controllers and Voltage Compensation in dq Domain

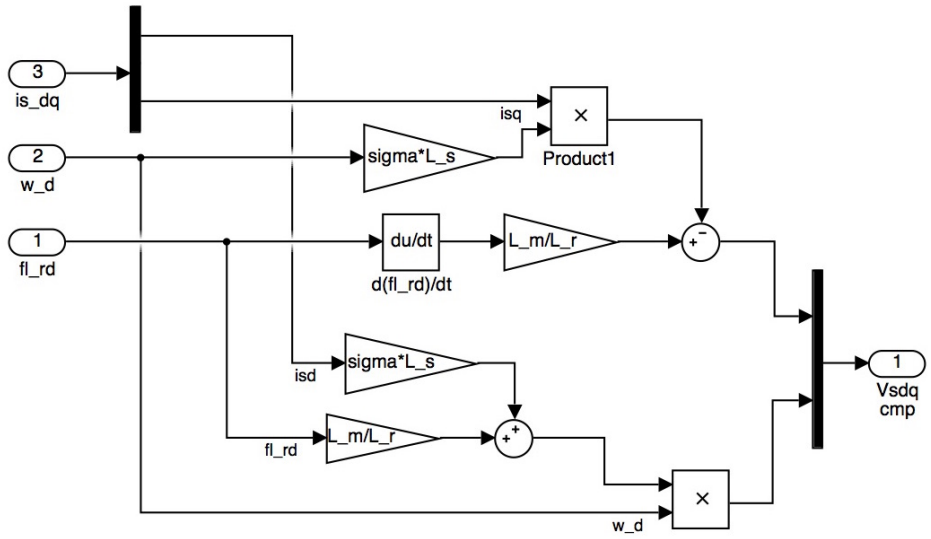

Figure 3: Model of Voltage Compensation

The simulation results obtained via our motor model in dq domain and those obtained via our motor model in three-phase frame constructed in Project 1 are shown in Fig. 4.

It can be recognized that our motor model in dq domain and the model in three-phase frame we constructed in Project 1 obtain the same results. It demonstrates that the the model in dq domain essentially is identical to the model in three-phase frame.

4.3.2 Simulation with and without Voltage Compensation

In this simulation, the machine is at the steady state with no load initially, and then the load torque with 3/4 rated value is applied. All parameters for the estimated motor model is accurate, which means that they are the same to those of the actual motor model. This simulation is conducted two times. One is with voltage compensation (the initial value of the integrator in the current loop is set to be $\boldsymbol{v}'_{s,dq}$), and the other one is without voltage compensation (the initial value of the integrator in the current loop is set to be $\boldsymbol{v}_{s,dq}$).

The simulation results obtained is shown in Fig. 5. From the simulation results, we can notice that it only has a limited influence on i_{sq} when no voltage compensation is utilized, whereas i_{sd} is impacted drastically without voltage compensation. As a result, there is limited influence on ω_{mech} and T_{em} but should be a drastic impact on B_r, as our analysis in Section 3.3 that i_{sq} is employed to deliver the desired electomganetic torque and that i_{sd} is employed to maintain the peak value of $\vec{B}_r$ at its rated value.

4.3.3 Simulation with Inaccurate Estimated Motor Parameters

In this simulation, three schemes are employed.

- Scheme 1: The estimated motor model has the same parameters to the actual motor model.
- Scheme 2: The rotor resistance in the estimated motor model is the half of the actual value.
- Scheme 3: The rotor leakage in the estimated motor model is 2 times the actual value.

Table 2: Parameter Comparison for Actual and Estimated Motor Model

	Actual Motor Model Estimated Model in Scheme 1	Estimated Model in Scheme 2	Estimated Model in Scheme 3
$L_r[H]$	0.0016	0.0016	0.0017
τ_r	1.6247	3.2495	1.7077
σ	0.1040	0.1040	0.1475

For the three schemes, three cases are conducted.

- Case 1: All parameters and initial values for the estimated motor, voltage compensation and controller modes are calculated based on inaccurate, estimated parameters.
- Case 2: All initial values for the voltage compensation, controller and estimated motor models are calculated based on accurate, actual parameters. All parameters for the the estimated motor and voltage compensation modes are calculated based on inaccurate, estimated parameters. All parameters for the controller mode are calculated based on accurate, actual parameters.
- Case 3: All initial values are calculated based on accurate, actual parameters. But all parameters for the estimated motor, voltage compensation and controller modes are calculated based on inaccurate, estimated parameters.
- Case 4: This case is the same to Case 3, except for that no voltage compensation model is employed in this case.

Similarly to the last simulation, the simulation starts at the steady state with rated load, and the load torque decreases to 0 at $t = 0.2$s and then increases to 3/4 rated value at $t = 1$s.

The simulation results are shown in Fig. 6, 7, 8 and 9, where $i_{sq,est}$ is calculated in the estimated motor model according to the output $\boldsymbol{i}_{s,abc}$ of the actual motor model, and where θ_{err} is obtained as

$$\theta_{err} = \theta_{da} - \theta_{da,est} \tag{4.64}$$

which is the gap between θ_{da} calculated in the actual motor model and $\theta_{da,est}$ calculated as θ_{da} in the estimated motor model.

From the simulation results, we can find that in all the three cases, the results obtained in Scheme 1 are quite similar to those obtained Scheme 3, except for i_{sq}. This means that 1 time increased estimated rotor leakage has limited influence on the control of θ_{da}, T_{em} and ω_{mech}. This conclusion also can be demonstrated from Table 2, from which we can find the estimated parameters in Scheme 3 are more close to the actual value. Besides, we can find that for i_{sq}, there is a big gap between Scheme 1 and Scheme 3, while the gap for θ_{err} is quite small. This demonstrates that the control effect is influenced by θ_{err} or the gap between i_{sq} and $i_{sq,est}$ more than the concrete value of i_{sq} or $i_{sq,est}$.

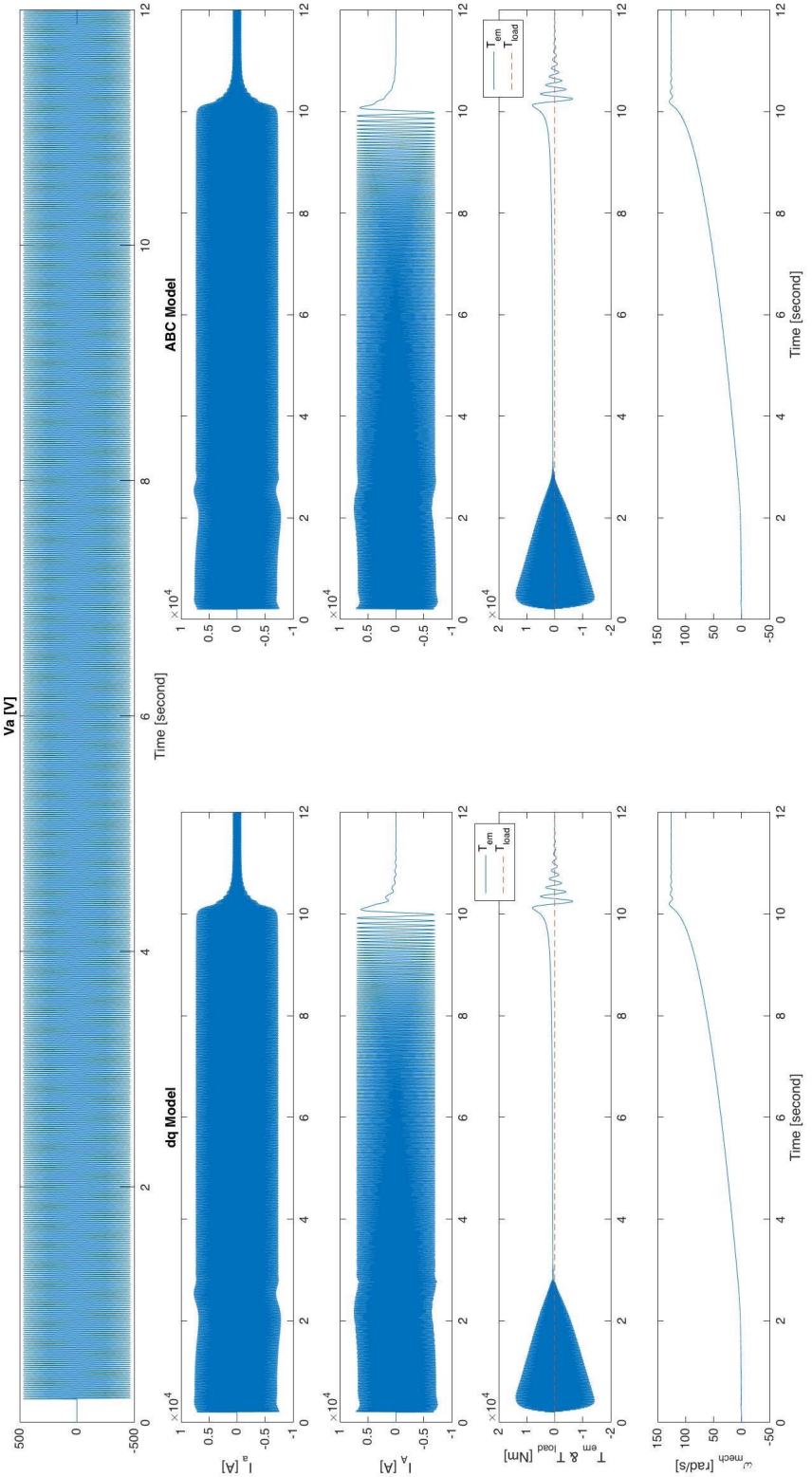

Figure 4: Simulation Results of Doing Line Start

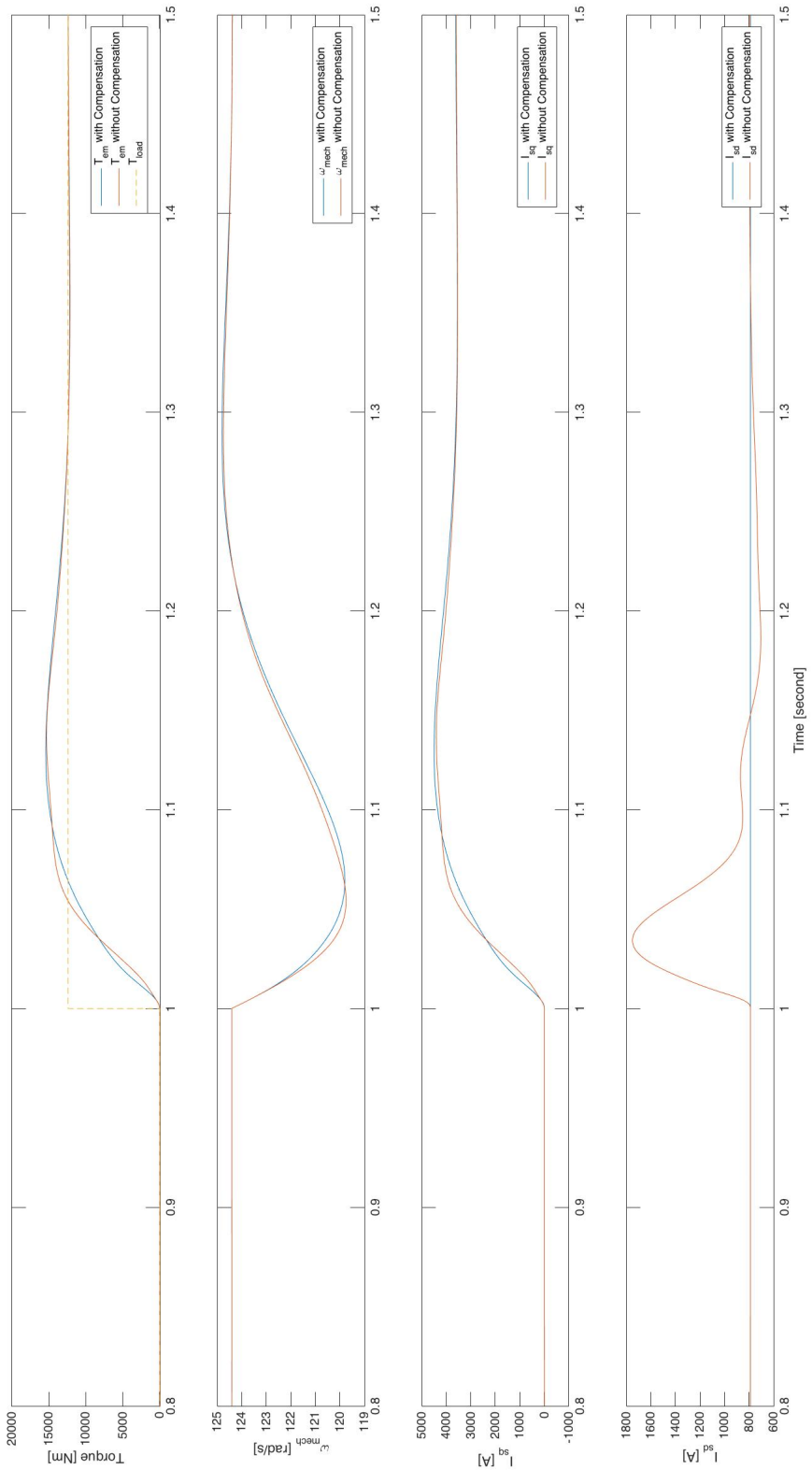

Figure 5: Comparison of Simulation with and without Voltage Compensation

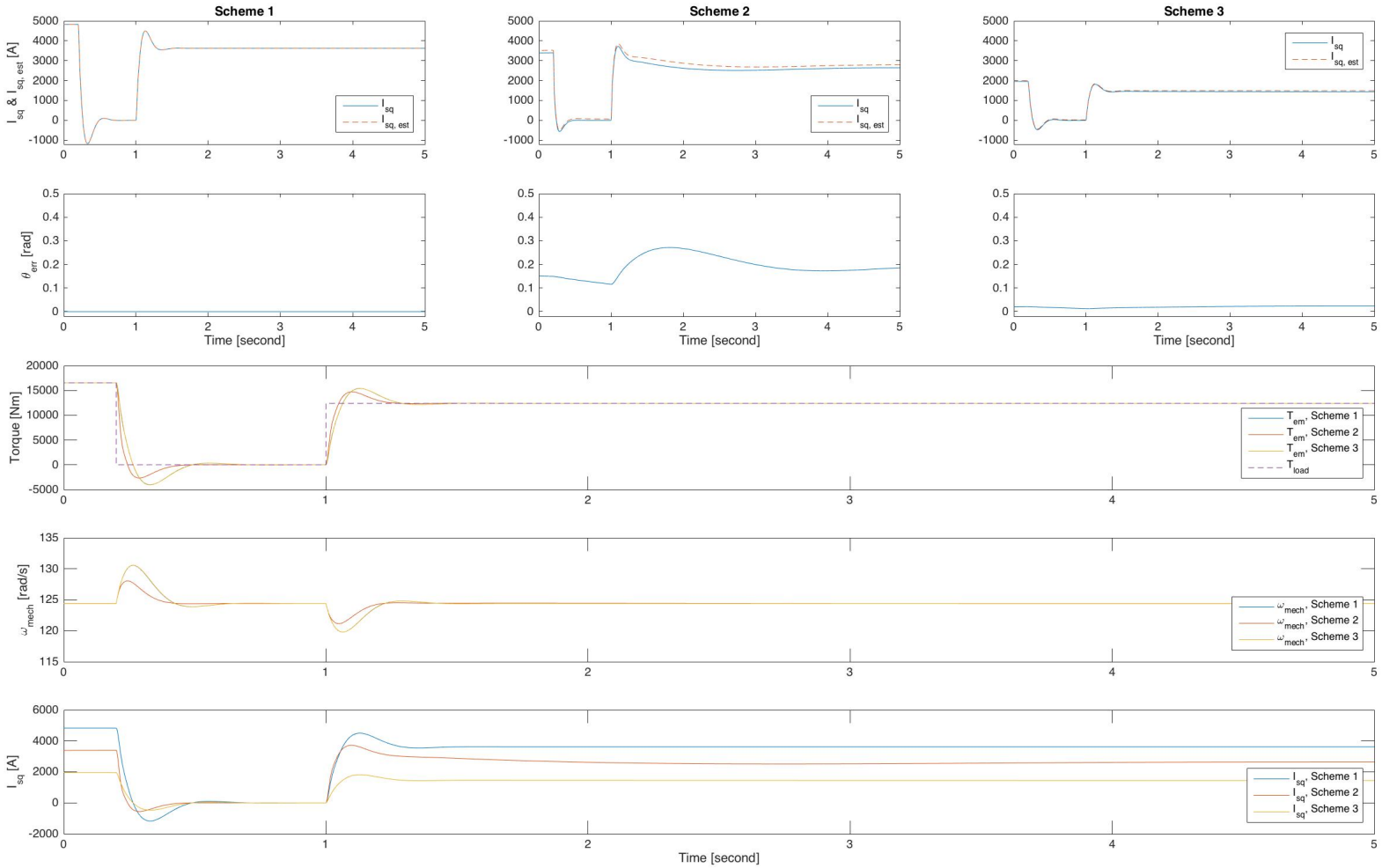

Figure 6: Simulation with Inaccurate Estimated Motor Model, Case 1

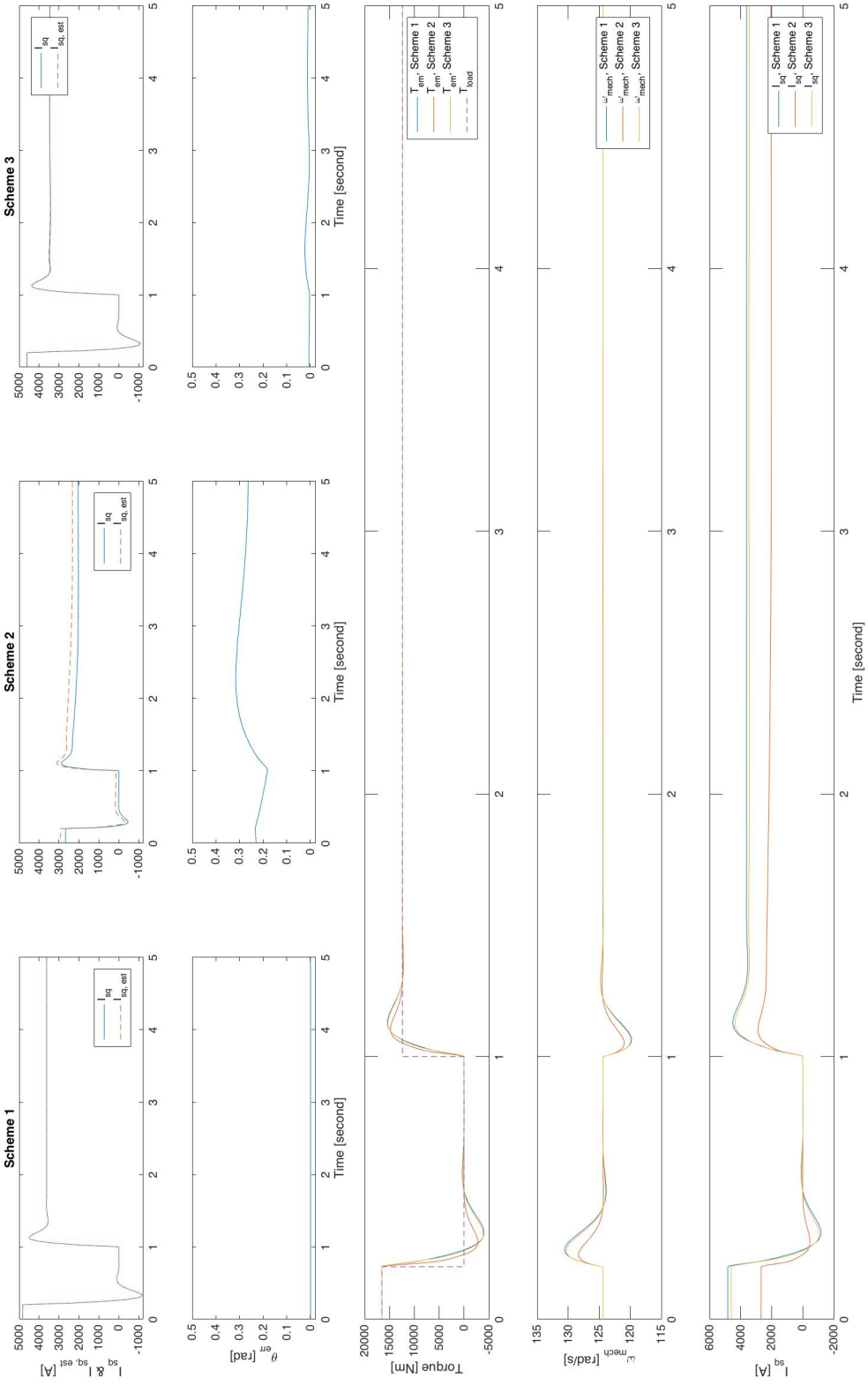

Figure 7: Simulation with Inaccurate Estimated Motor Model, Case 2

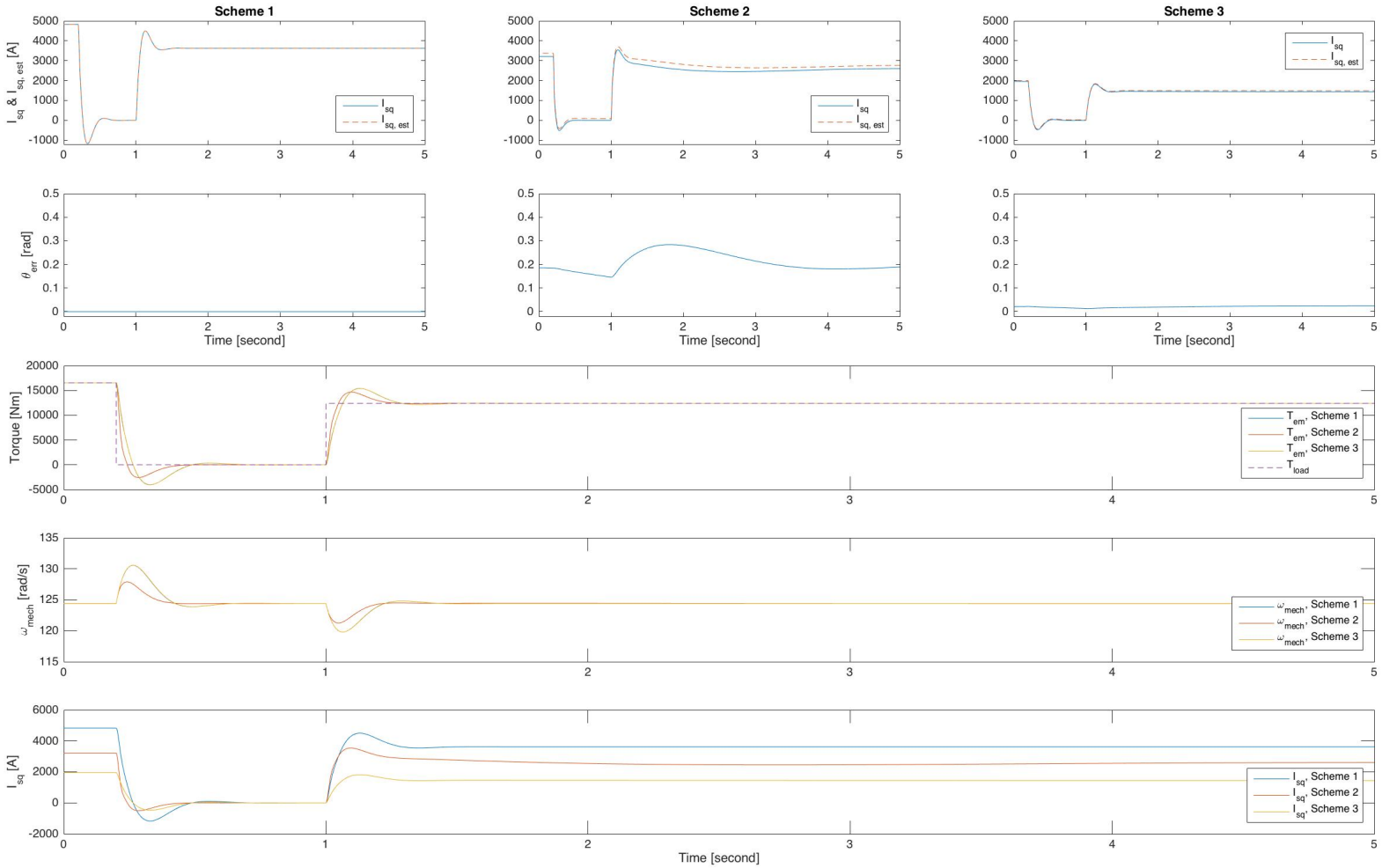

Figure 8: Simulation with Inaccurate Estimated Motor Model, Case 3

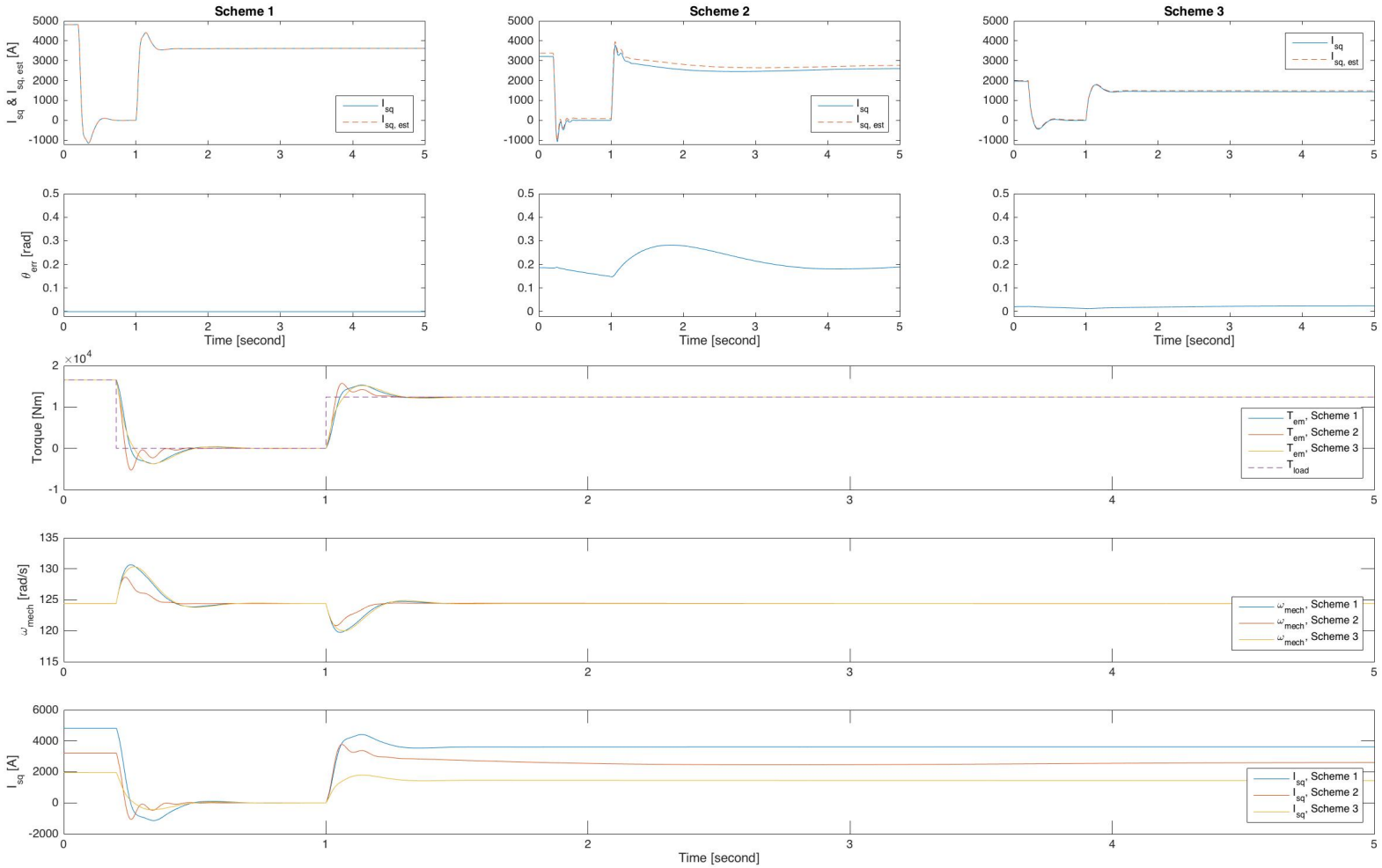

Figure 9: Simulation with Inaccurate Estimated Motor Model, Case 4

Comparing Case 1 and Case 3, we can recognize that after the system reaches steady state, the difference in initial values has very limited impact on the control effect.

Comparing Case 2 and Case 3, we can recognize that when facing inaccurate estimated motor model, controllers designed in accordance with accurate motor parameters can lead to a better control effect and more accurate control on i_{sq}.

Comparing Case 3 and Case 4, we can recognize that the control effect when voltage compensation models are employed are much better than that when no voltage compensation model is employed. Contrasting the result to the simulation in Section 4.3.2, we can reach the conclusion that voltage compensation can effectively improve the control effect when we cannot obtain accurate motor parameters.

Besides, it can be spotted that in the three schemes and four cases, controllers always are able to keep ω_{mech} at its rated value. This means that the adopting inaccurate, estimated parameters cannot influence the final control effect of controllers.

5 Conclusion

In this project, an induction machine model in *dq* domain is built up in theory as well as in MATLAB/Simulink. From simulation, it is proven that the model in *dq* domain is identical essentially to the model in three-phase frame, i.e. to the model built in Project 1. This means that it is an effective method to analyze induction machines via *dq* domain.

Then, from simulation in Section 4.3.2, we find that the lack of voltage compensation model has a limited influence on the control over the rotor rotational speed ω_{mech} when we have accurate motor parameters, but a relatively drastic influence on i_{sd} as well as the peak value of rotor flux $\vec{B}_r$. However, with inaccurate motor parameters, voltage compensation can effectively ameliorate the control effect, as the analysis in Section 4.3.3.

Besides, from simulation in Section 4.3.3, it is demonstrated that the inaccurate parameters of the estimated motor model could result in unideal control effect; however, the controllers still are able to adjust the rotor rotational speed ω_{mech} to keep it as its rated value, even if the parameters of the controllers are calculated according to the inaccurate, estimated parameters. And, the difference in control effects is depended more on θ_{err} or the gap between i_{sq} and $i_{sq,est}$.

References

[1] N. Mohan, *Electric Machines and Drives*. 2012.

[2] N. Mohan, *Advanced Electric Drives: Analysis, Control, and Modeling Using MATLAB/Simulink®*. 2014.